Available online at www.sciencedirect.com
SCIENCE DIRECT®
Journal of Nuclear Materials 329–333 (2004) 1365–1369
journal of nuclear materials
www.elsevier.com/locate/jnucmat

Experimental study of cracking methane by Ni/SiO_2 catalyst

S. Fukada *, N. Nakamura, J. Monden, M. Nishikawa

Department of Applied Quantum Physics and Nuclear Engineering, Kyushu University, 6-10-1, Hakozaki, Higashi-ku, Fukuoka 812-8581, Japan

Abstract

Rates of CH_4 cracking on a Ni/SiO_2 composite catalyst in a flow-through system were determined as a function of a flow rate, the CH_4 concentration in carrier, temperature and the amount of carbon deposits. The CH_4 decomposition reaction was of the first-order, and its rate constant was independent of the flow rate and the inlet CH_4 concentration. Values of the steady-state decomposition rate constant were correlated to $k_{\mathrm{decomp}} = 3.09 \times 10^1 \exp(-29.5[\mathrm{kJ/mol}]/R_{\mathrm{g}}T)$ [s^{-1}]. The overall decomposition rate gradually decreased with an increase in the amount of carbon deposits in the catalyst bed. The history of the CH_4 decomposition was discussed in terms of an increase in the linear velocity through the bed and an increase in interference with catalytic performance on Ni. Regeneration of the catalyst was compared under two purge gas conditions between H_2 and O_2. It was found that the H_2 purge was more efficient.

1. Introduction

Tritiated methane will be generated from plasma–wall interaction when high-temperature plasma of hydrogen isotopes, deuterium and tritium, is burning in a nuclear fusion reactor. A burn-up ratio of tritium will not be so high that unburned fuel should be recycled to the reactor after fuel purification and impurity processing. There are several ways proposed to recover tritium from exhaust fuel. They are permeation, catalytic decomposition, catalytic oxidation, gettering and so on [1,2]. Tritiated methane can be cracked into carbon and tritium on surfaces of Ni or precious metals at moderate temperatures. A process of the catalytic decomposition combined with tritium permeation was proposed for the ITER fuel processing loop [3,4]. There were many deviations in previous data on decomposition rate [5]. In addition, there were less studies giving catalytic decomposition rates as a function of temperature, flow rate and carrier gas conditions necessary for the design of a catalyst bed, while some researches using tritiated methane were performed [6,7]. In the present study, variations of the CH_4 concentration between the inlet and outlet of a Ni/SiO_2 composite catalyst bed were determined in a flow-through system as a function of the inlet CH_4 concentration, flow rate, temperature and the amount of carbon deposits. The results under two different carrier gas conditions of Ar and H_2 were compared. The Ar carrier simulated a condition of the low hydrogen isotope concentration and the H_2 one did that of the high concentration. Repeated use of Ni catalysts is an issue to be proved for application to a loop of the fuel purification system. Therefore, H_2 purge for regeneration of Ni catalysts was compared with O_2 purge.

2. Experimental

Fig. 1 shows a schematic diagram of the experimental apparatus. Gases of CH_4, H_2, O_2 and Ar were supplied from gas cylinders with purity of greater than 99.999%. The volumetric flow rate regulated by their respective mass-flow meters ranged from 5 cm^3 (NTP)/min to 500 cm^3 (NTP)/min. The superficial contact time varied from 0.1 to 10 s. The total pressure at the bed outlet, p_t, was atmospheric one. The gas lines were made of a 316 stainless-steel tube with inner diameter of 1.6 mm and

* Corresponding author. Tel.: +81-92 642 4140; fax: +81-92 642 3800.
E-mail address: sfukada@nucl.kyushu-u.ac.jp (S. Fukada).

0022-3115/$ - see front matter © 2004 Elsevier B.V. All rights reserved.
doi:10.1016/j.jnucmat.2004.04.199

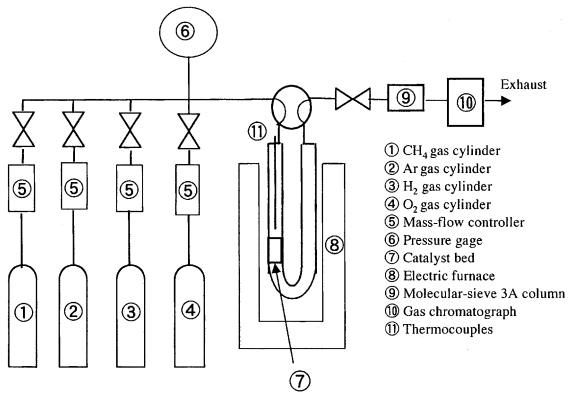

Fig. 1. A schematic diagram of the experimental apparatus.

the catalyst column was made of a quartz-glass tube with inner diameter of 6.3 mm. The Ni/SiO_2 composite catalyst of 0.50 or 1.00 g with diameter of 20–60 mesh (0.25–0.83 mm) was treated by purge of purified O_2, then purified H_2 and finally purified Ar for sufficient time. Then, a constant concentration of a mixture of CH_4 and balance gas (Ar or H_2) was introduced into the catalyst bed. In regeneration, the gas line was changed to H_2 or O_2 purge flow after three hours exposure to the Ar–CH_4 flow under a constant flow rate. The concentrations of H_2, CH_4, O_2, CO, CO_2 and other hydrocarbons were detected by gas chromatography that could measure around 10 ppm of their respective component concentrations.

A scanning electron microscope (SEM) photo of the catalyst showed that small Ni particles distributed uniformly in pellets composed of SiO_2 substrates [8]. The contents of the composite catalyst determined by an electron dispersive X-ray fluorescence spectrometer were NiO; 67.7%, SiO_2; 24.3%, CuO; 2.85%, Al_2O_3; 2.04%, Cr_2O_3; 1.91%, Fe_2O_3; 0.425, Co_2O_3; 0.355%, K_2O; 0.305%, MnO; 0.104%.

3. Definition of overall methane decomposition rate constant

CH_4 molecules in a bulk flow diffuse through balance gas and in porous catalyst particles, stick on Ni surfaces, and finally decompose to carbon and hydrogen atoms. The overall CH_4 cracking reaction is expressed as $CH_4 = C + 2H_2$. There seemed to be no chance of the formation of Ni carbide under the present experimental condition judging from the ΔG value of the reaction, $CH_4 + 3Ni = Ni_3C + 2H_2$ [9]. We could not find any traces of the Ni_3C phase in the X-ray diffractometry analysis of the Ni/SiO_2 composite catalyst after use.

The ratio of the outlet CH_4 partial pressure to the inlet one, $p_{CH_4,out}/p_{CH_4,in}$, is called a CH_4 concentration ratio in the present study. The overall reaction rate constant, k_{decomp}, through the catalytic bed was defined as follows:

$$k_{\mathrm{decomp}} = \frac{W}{V} \ln\left(\frac{p_{\mathrm{CH_4,in}} - p_{\mathrm{CH_4,s}}}{p_{\mathrm{CH_4,out}} - p_{\mathrm{CH_4,s}}}\right), \tag{1}$$

where V is the volume of the catalytic bed and W is the volumetric flow rate at the bed inlet. The ratio of W/V has a unit of s^{-1} (or h^{-1}) and is usually called a superficial velocity in the chemical engineering field. The reciprocal of the superficial velocity is superficial contact time. The latter part of Eq. (1) is a logarithmic mean of a driving force of the CH_4 decomposition. There were two possibilities whether the rate-determining step is diffusion in a gaseous phase or intrinsic decomposition reaction on Ni. The step was determined experimentally from the dependence of the CH_4 concentration ratio or the overall rate constant on the flow rate, carrier gas condition and the inlet CH_4 concentration.

The partial pressure of CH_4 on catalyst surfaces, $p_{CH_4,s}$, in Eq. (1) was determined from the mass-action law of the decomposition reaction

$$K_p = \frac{p_{\mathrm{H_2,s}}^2}{p_{\mathrm{CH_4,s}}} = \exp\left(-\frac{\Delta G}{R_g T}\right). \tag{2}$$

The calculated value of $p_{CH_4,s}$ in the Ar–CH_4 system was negligibly small compared to $p_{CH_4,in}$. On the other hand, $p_{CH_4,s}$, in the H_2–CH_4 system was equal to $p_t - p_{H_2,s}$. The present system is an isobaric one. Therefore the partial pressure of CH_4 or H_2 was in proportion to the molar fraction of each component.

4. Results and discussion

4.1. Effects of balance gas

The outlet concentrations of CH_4 and H_2 reached their respective steady-state values immediately after the supply of a mixture of CH_4 and balance gas. Any other gas species were not detected at the outlet. Fig. 2 shows variations of the CH_4 concentration ratio with different inlet CH_4 concentrations under the same flow rate (30 cm^3 (NTP)/min) for the Ar–CH_4 system. The vertical axis of the left-hand side shows values of the CH_4 concentration ratio, $x_{CH_4,out}/x_{CH_4,in}$, and that of the right-hand side does the ratio of the outlet H_2 molar fraction to the inlet CH_4 one. The stoichiometric relation of $1 - x_{CH_4,out}/x_{CH_4,in} = x_{H_2,out}/2x_{CH_4,in}$ was observed experimentally. Therefore, a CH_4 molecule split to a carbon and two H_2 molecules without any time lag under the steady-state condition.

In the Ar–CH_4 system, the CH_4 concentration ratio was independent of the inlet CH_4 concentration.

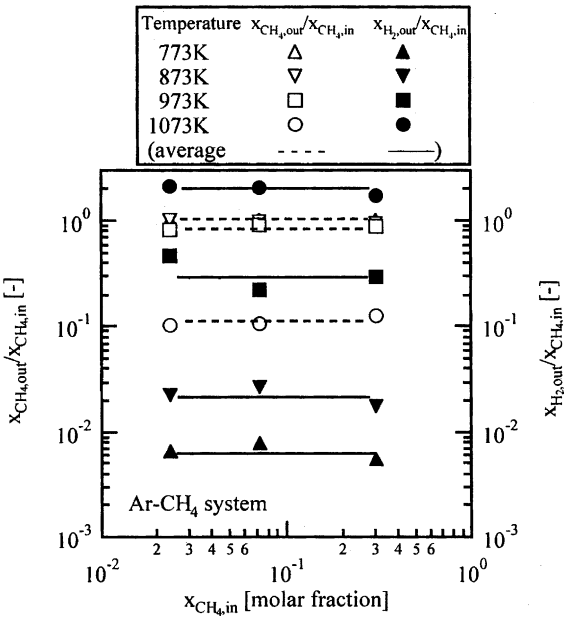

Fig. 2. Variations of the CH_4 concentration ratio with the inlet CH_4 concentration.

Therefore the apparent decomposition reaction was of the first-order. The concentration ratio increased with elevating temperature. On the other hand, the decomposition behavior in the H_2–CH_4 system showed differently. The CH_4 decomposition under the conditions where $x_{CH_4,in} > 0.3$ and $T > 900$ K occurred in a similar way to the Ar–CH_4 system. However, no decomposition occurred when $x_{CH_4,in} < 0.3$. This was because the inlet condition in the latter case was greater than the equilibrium value of Eq. (2). Thus, the driving force defined in Eq. (1) was considered reasonable regardless of different carrier gas conditions. Consequently, it was found that the condition of the lower H_2 concentration was preferable to CH_4 decomposition.

4.2. Effects of flow rate and temperature

Fig. 3 shows dependence of the ratios, $x_{CH_4,out}/x_{CH_4,in}$ and $x_{H_2,out}/x_{CH_4,in}$, on the flow rate or the superficial velocity under the same inlet CH_4 concentration. As seen in the figure, the concentration ratio was in proportion to the reciprocal of the flow rate in the wide range. So, the overall decomposition rate constant defined was a unique function of only temperature independent of the flow rate and the inlet CH_4 concentration.

Fig. 4 shows the result of the CH_4 decomposition rate constant versus the reciprocal of the column temperature. Thus, the rate constant determined were correlated to the following Arrhenius relation:

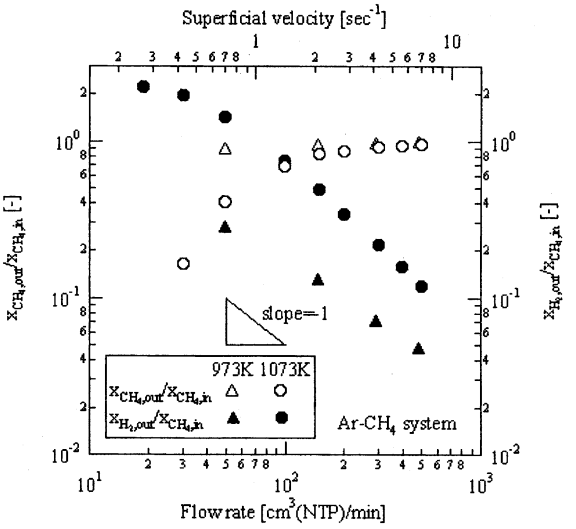

Fig. 3. Dependence of CH_4 and H_2 concentration ratios on gas flow rate.

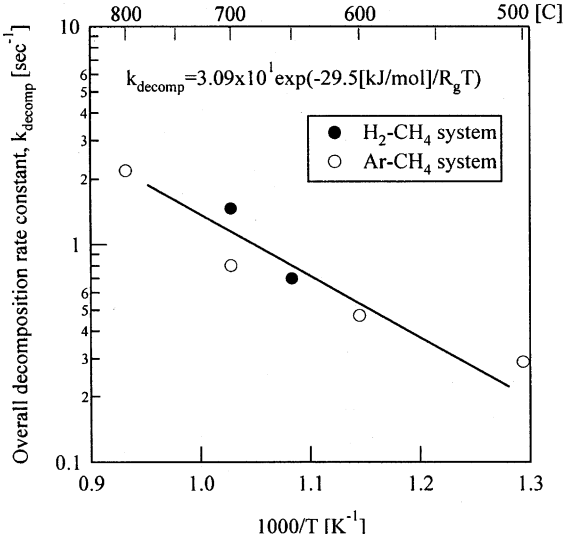

Fig. 4. Dependence of overall CH_4 decomposition rate constant on temperature.

$$k_{\text{decomp}} = 3.09 \times 10^{1} \exp(-29.5\ [\text{kJ/mol}]/R_g T) \quad [\text{s}^{-1}]. \tag{3}$$

If the rate-determining step were diffusion in the gas phase, the decomposition rate in the H_2–CH_4 system should be higher than the Ar–CH_4 system, because the diffusion coefficient of CH_4 in balance gas is different between Ar and H_2. However, there were no differences in not only the experimental k_{decomp} value but also its activation energy between the two systems. Consequently, we could conclude that the rate-determining

step was not diffusion in the gaseous phase but the intrinsic CH_4 decomposition reaction. The activation energy of the CH_4 decomposition reaction determined here was a little greater than that of the sticking coefficient on Ni(1 0 0) surfaces of a single crystal (27 kJ/mol) and a much smaller than that on Ni(1 1 1) surfaces (53 kJ/mol) [5]. Consequently, it was considered that both of the two sites gave reaction places to the present cracking process.

4.3. Long-time experiment

Fig. 5 shows two examples of the variations of the CH_4 concentration ratio with the amount of carbon deposits at 873 K. The CH_4 concentration ratio was constant during a certain time after the gas supply. With time elapsing or an increase in the amount of carbon deposits, the CH_4 concentration ratio started increasing gradually. It was considered that there were two reasons for that. One was interference with the catalytic reaction on Ni particles by carbon deposits. The second was because of choking due to a decrease in flow area and so the increase of the linear velocity in the catalyst bed. However, the second reason was found to lead to deterioration of catalyst appearing immediately after the start of the gas supply. Since an induction time was observed in the deterioration of the catalytic behavior, there was higher possibility in the interference with Ni by carbon deposits.

The curves of the concentration ratio showed a similar history regardless of different inlet CH_4 concentrations. The amount of carbon deposits until the bed

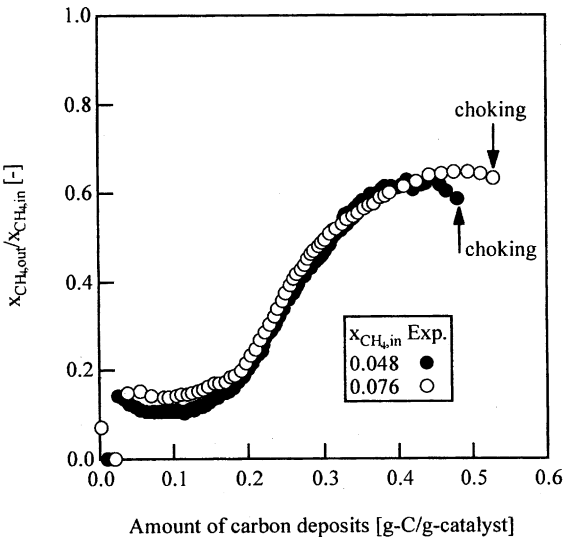

Fig. 5. Variations of the CH_4 concentration ratio with amount of carbon deposits.

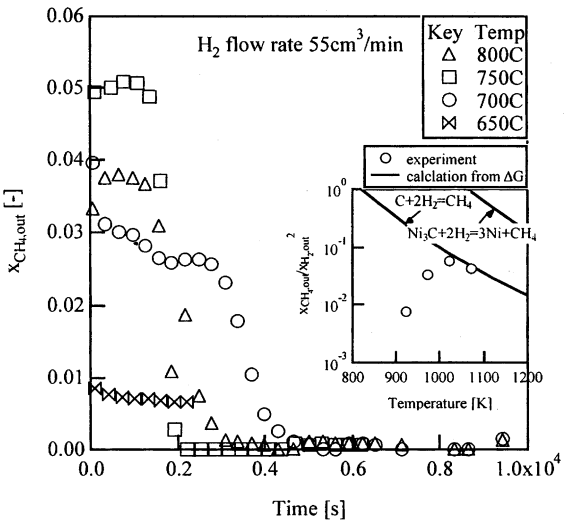

Fig. 6. Experimental results of removal of carbon deposits by H_2 purge.

was choked completely was almost the same regardless of different feed conditions.

4.4. Regeneration of Ni/SiO_2 catalyst

Recovery of carbon and regeneration of the Ni/SiO_2 catalyst were compared between the two ways of H_2 purge and O_2 purge between 573 and 1073 K. So that, almost all of carbon deposits were removed from the catalyst bed by H_2 purge at 773–1073 K as shown in Fig. 6. The outlet CH_4 concentration reached a constant value immediately after the H_2 purge. The concentration depended on temperature. Especially, its value for $T > 1000$ K was consistent with one determined from the ΔG value of $CH_4 = C + 2H_2$. Any other component except for CH_4 was not detected at the outlet. Carbon, on the other hand, could not removed by O_2 purge. Any traces of CO, CO_2 and $Ni(CO)_4$ were not detected at the bed outlet or in the XRD spectrum by O_2 purge less than 773 K. We could not see any loss of the amount of the Ni/SiO_2 catalyst after long-time exposure to the CH_4 flow.

5. Conclusions

The decomposition rate of CH_4 through the Ni/SiO_2 composite catalyst bed was determined as a function of the inlet CH_4 concentration, the carrier gas condition, the flow rate and temperature experimentally. The decomposition reaction was of the first-order and the overall decomposition rate constant was independent of the flow rate and the balance gas condition. The acti-

vation energy of the overall decomposition reaction was 29.5 kJ/mol. Carbon deposited in the catalyst bed was removed by H_2 purge.

References

[1] S. Fukada, Hydrogen Isotope Separation by Hydrogen-Absorbing-Alloy Beds, NTS, 2000 (in Japanese).
[2] S. Fukada, J. Plasma Fus. Res. 76 (2000) 1036.
[3] M. Glugla, R.-D. Penzhorn, Fus. Eng. Des. 28 (1995) 348.
[4] H. Yoshida, O. Kveton, J. Koonce, D. Holland, R. Haange, Fus. Eng. Des. 39&40 (1998) 875.
[5] T.P. Beebe Jr., D.W. Goodman, B.D. Kay, J. Chem. Phys. 87 (1987) 2305.
[6] M. Glugla, R.D. Penzhorn, J.L. Anderson, J.R. Bartlit, Fus. Technol. 14 (1988) 683.
[7] S. Fukada, J. Nucl. Sci. Technol. 38 (2001) 273.
[8] S. Fukada, N. Nakamura, J. Monden, Int. J. Hydrogen Energy 29 (2004) 619.
[9] O. Kubaschewski, C.B. Alcock, Metallurgical Thermo-Chemistry, 5th Ed., Pergamon, New York, 1979.